Ticks and Tick-borne Diseases 13 (2022) 102024

Contents lists available at ScienceDirect

Ticks and Tick-borne Diseases

journal homepage: www.elsevier.com/locate/ttbdis

Original article

Rhipicephalus linnaei (Audouin, 1826) recognised as the "tropical lineage" of the brown dog tick *Rhipicephalus sanguineus* sensu lato: Neotype designation, redescription, and establishment of morphological and molecular reference

Jan Šlapeta [a,*], Bruce Halliday [b], Shona Chandra [a], Abdullah D. Alanazi [c], Sobhy Abdel-Shafy [d]

[a] Sydney School of Veterinary Science, Faculty of Science, University of Sydney, Sydney, New South Wales 2006, Australia
[b] Australian National Insect Collection, CSIRO, GPO Box 1700, Canberra, Australian Capital Territory 2601, Australia
[c] Department of Biological Sciences, Faculty of Science and Humanities, Shaqra University, Ad-Dawadimi, Saudi Arabia
[d] Department of Parasitology and Animal Diseases, Veterinary Research Institute, National Research Centre, Dokki, Giza, Egypt

ARTICLE INFO

Keywords:
WGS
Mitogenome
mtDNA
Morphological re-description
Neotype
Nomenclature

ABSTRACT

We re-describe the adult stages of *Rhipicephalus linnaei* (Audouin, 1826), and characterise its diagnostic molecular traits. A male *R. linnaei* collected in Esna City, Luxor Governorate, Egypt is designated as the neotype. *Rhipicephalus linnaei* is re-established as a valid tick name and removed from the synonymy list of *Rhipicephalus sanguineus* (Latreille, 1806). *Rhipicephalus linnaei* is most similar to *R. sanguineus* and *Rhipicephalus camicasi* Morel, Mouchet & Rodhain, 1976 because they share similar elongated comma-like spiracula that are narrowly visible dorsally, and the dorsal prolongation is narrower than the width of the adjacent festoon. The male of *R. camicasi* is distinguished from *R. linnaei* by the non-tapering caudal widening of the spiracula. The male of *R. sanguineus* is distinguished from *R. linnaei* by shorter extension that does not taper into a long narrow extension of the spiracula. The genital pore atrium of female *R. linnaei* is broadly U-shaped, while it is a narrower U-shape in *R. sanguineus*. The remaining species within the *R. sanguineus* species complex – *Rhipicephalus sulcatus* Neumann, 1908, *Rhipicephalus turanicus* Pomerantsev, 1940, *Rhipicephalus guilhoni* Morel & Vassilades, 1963, *Rhipicephalus secundus* Feldman-Muhsam, 1952 and *Rhipicephalus afranicus* Bakkes, 2020, all exhibit spiracula with the dorsal prolongation as wide as the adjacent festoon. The DNA sequence of *R. linnaei* is most closely related to *R. guilhoni*. The phylogenetic analysis of mitogenome (mtDNA) sequences including assembled mtDNA from whole genome sequencing of the neotype supports *R. linnaei* as a well-defined taxon when compared with DNA sequences of other species of the *R. sanguineus* species complex, in particular: *R. sanguineus, R. turanicus, R. secundus* and *R. camicasi.* Molecularly, *R. linnaei* belongs to the so-called *R. sanguineus* s.l. "tropical lineage" distributed globally including the Americas, Africa, Europe, Asia and is the only species from *R. sanguineus* species complex in Australia.

1. Introduction

The brown dog tick, *Rhipicephalus sanguineus* sensu lato (s.l.), is an important tick whose significance is associated with its capacity to transmit devastating vector borne diseases, including canine ehrlichiosis caused by *Ehrlichia canis* (Neave et al., 2022; Moraes-Filho et al., 2015). The taxon *R. sanguineus* s.l. is generally agreed to be a species complex of several well and not so well-defined species using traditional morphology (Walker et al., 2000; Gray et al., 2013; Nava et al., 2015, 2018; Bakkes et al., 2020). These include *Rhipicephalus sanguineus* (Latreille, 1806), *Rhipicephalus sulcatus* Neumann, 1908, *Rhipicephalus turanicus* Pomerantsev, 1940, *Rhipicephalus secundus* Feldman-Muhsam, 1952, *Rhipicephalus guilhoni* Morel & Vassilades, 1963, *Rhipicephalus camicasi* Morel, Mouchet & Rodhain, 1976, *Rhipicephalus afranicus* Bakkes, 2020, among others (Walker et al., 2000). While morphological discrimination is possible in some situations, the availability of molecular techniques has further supported discrimination of the individual cryptic species and vice versa enables the resurrection of others (Nava

* Corresponding author.
E-mail address: jan.slapeta@sydney.edu.au (J. Šlapeta).

https://doi.org/10.1016/j.ttbdis.2022.102024
Received 16 March 2022; Received in revised form 15 July 2022; Accepted 29 July 2022
Available online 9 August 2022

et al., 2018; Chandra et al., 2022; Mumcuoglu et al., 2022). When *R. sanguineus* sensu stricto (s.s.) was recently redescribed, the authors argued that the diagnostic features and differentiation from the related species is challenging, citing "*morphological diagnoses of ticks from this group will continue to be difficult, and molecular characterization of all species should be obtained to support morphological identifications*" (Nava et al., 2018). Extensive surveys of DNA sequence data obtained over the past decade demonstrated that a cryptic genetic lineage known informally as *R. sanguineus* s.l. "tropical lineage", is the most frequently recorded lineage globally yet does not have a formal name (Šlapeta et al., 2021). *Rhipicephalus linnaei* (Audouin, 1826) within the synonymy of *R. sanguineus* was considered the oldest name and proposed to be used for *R. sanguineus* s.l. "tropical lineage" (Šlapeta et al., 2021). Besides *R. sanguineus* s.l. "tropical lineage" it has previously been referred to as *Rhipicephalus* sp. I, "tropical species" or "northern lineage" (Moraes-Filho et al., 2011; Chitimia-Dobler et al., 2017; Hornok et al., 2017; Nava et al., 2018). In fact, Moraes-Filho et al. (2011) were the first to suggest separation of "tropical" species within Latin America and globally using partial mitochondrial 16S rDNA sequences.

In 2021, we argued that there was no exceptional need to designate a neotype for *R. linnaei* citing Article 75 (ICZN, 1999), because the material we associated with the name was formerly known as the "tropical lineage" of *R. sanguineus* s.l. (ICZN, 1999, Article 75.3. Qualifying conditions). Recently, however, Mumcuoglu et al. (2022) considered *R. linnaei* as *nomen dubium* citing *"populations of ticks not formally described which are grouped under the names* R. sanguineus *s.l. "tropical lineage" sensu Nava et al. (2018) (the name Rhipicephalus linnaei (Audouin, 1826) used by Šlapeta et al. (2021) to formally designate to the taxon* R. sanguineus *s.l. "tropical lineage" is considered here a nomen dubium following Guglielmone et al. (2015 and updates)"*. Guglielmone et al. (2015 and updates) considered that the lack of material of *Ixodes linnaei* to be compared invalidates any attempt to resuscitate the name, in other words they suggested that there is no scientific support for such decision, or simply, words are not equivalent to a specimen. The above demonstrated that to clarify the identity of *R. linnaei*, a neotype needs to be designated and described to satisfy Article 75 (ICZN, 1999) and the needs of the scientific community.

The aim of this study was to collect extant material of *Rhipicephalus sanguineus* s.l. from Egypt, the type locality of *R. linnaei*. A neotype is described for *R. linnaei* from a series of vouchers that are morphologically and genetically characterised to clarify the status of *R. sanguineus* s.l. "tropical lineage".

2. Material and methods

2.1. Material collection

Ticks from dogs ($n = 21$), *Canis lupus familiaris*, were collected from Esna City, Luxor Governorate, Egypt (25°17′36.0″N 32°33′23.0″E; 25.293333, 32.556389), during the last week of October 2021, by Sobhy Abdel-Shafy. Ticks in pools (1–5 ticks) per dog were stored in 70% ethanol after collection. Ticks collected were of varying developmental stages (2 nymphs, 32 adults) and varying levels of engorgement (Supplementary Table S1).

2.2. Morphological identification

All ticks were morphologically identified using a stereo microscope (SMZ-2B, Nikon, Australia) using various keys and guides (Roberts, 1965; Walker et al., 2000). Morphologically important features were more closely visualised and photographed using a digital microscope (VHX-6000, KEYENCE Inc., Japan). The key characters described were observed, measured and recorded using a calibrated VHX-6000 digital microscope (Supplementary Table S2), as previously described (Chandra et al., 2020, 2021). Body measurements (exclusive of capitulum) was measured from apices of scapulae to posterior margin of the sixth festoon.

2.3. DNA isolation

All unengorged ticks and selection of engorged ticks were selected for DNA isolation. Using a sterile single use no. 11 scalpel blade, an incision was made to individual tick idiosoma prior to drying in a sterile 1.5 ml Eppendorf tube on a heat block. Dried ticks with incisions in their idiosoma were used for total tick genomic DNA (gDNA) isolation with the Monarch Genomic DNA Purification Kit (New England Biolabs, Australia). Following the overnight protein lysis with Proteinase K, the liquid phase was transferred and gDNA isolated following manufacturer's instructions, while the exoskeleton was retained and preserved in 70% (v/w) ethanol. Extracted gDNA was stored at −20 °C.

2.4. Amplification of the mitochondrial cox1, 16S rRNA and 12S rRNA genes

The ~600 nucleotide (nt) fragment of the mitochondrial DNA (mtDNA) cytochrome c oxidase subunit I (*cox*1) gene was amplified using the following primer sets: LCO1490/HCO2198 and S0725/S0726 as described in Chandra et al. (2019). Modified cycling conditions were utilised to increase the efficiency of amplification following with S0725/S0726 and S0725/HCO2198. The cycling conditions were adopted from Meiklejohn et al. (2019) and included 95 °C for 2 min, followed by 5 cycles of 94 °C for 15 s, 45 °C for 15 s, 72 °C for 15 s, followed by 35 cycles of 94 °C for 15 s, 51 °C for 15 s, 72 °C for 15 s and a final extension of 72 °C for 5 min. The fragments of the 16S ribosomal RNA (rRNA) and 12S rRNA gene were amplified in a conventional PCR using the primer sets: S0749/S0750 (Black and Piesman, 1994) and S0738_T1B/S0739_T2A (Beati and Keirans, 2001), respectively, as previously described (Chandra et al., 2019). MyTaq™ Red Mix (Bioline, Australia) was used for DNA amplifications in 30 µl reactions, with 2µl of template gDNA. All reactions included PCR-grade water (ddH_2O) as a no template control. The PCR reactions were performed in a T100™ Thermal Cycler (BioRad, Australia) and the PCR products were sequenced at Macrogen Ltd. (South Korea).

2.5. Whole genome sequencing of Rhipicephalus linnaei and assembly of mitogenome from next generation sequence data

The gDNA isolated from an adult *R. linnaei* was used for next-generation sequencing (NGS) using NEBNext® DNA Library Prep Kit followed by NGS using 150 bp paired end Illumina sequencing system at a depth of 1Gb of raw sequence data (Novogene, Singapore). The whole mtDNA was assembled from FastQ data using the MITObim pipeline (Hahn et al., 2013) [https://github.com/chrishah/MITObim] with the aid of the DNA sequence obtained from Šlapeta et al. (2021). The circular mtDNA was confirmed by the presence of overlapping ends of the assembly. The assembly was repeated three times with varying percentages of the raw FastQ sequence data (10–25%), keeping mtDNA coverage at 60–100×. The obtained mtDNA was annotated with the aid of MITOS Web Server (Bernt et al., 2013) [http://mitos.bioinf.uni-leipzig.de/] and aligned with available complete mtDNA sequences of species of *Rhipicephalus* in CLC Main Workbench 21 (CLC bio, Qiagen, Australia) for manual validation, which included all available mitogenomes of *R. sanguineus* s.l. group (Šlapeta et al., 2021; Chandra et al., 2022).

2.6. Phylogenetic analysis

Sequence alignments were constructed using CLC Main Workbench 21 (CLC bio, Qiagen, Australia). Evolutionary analyses including selection of models were conducted in MEGA 11 (Tamura et al., 2021) [https://www.megasoftware.net/].

Whole mitogenome sequence alignments were included for newly

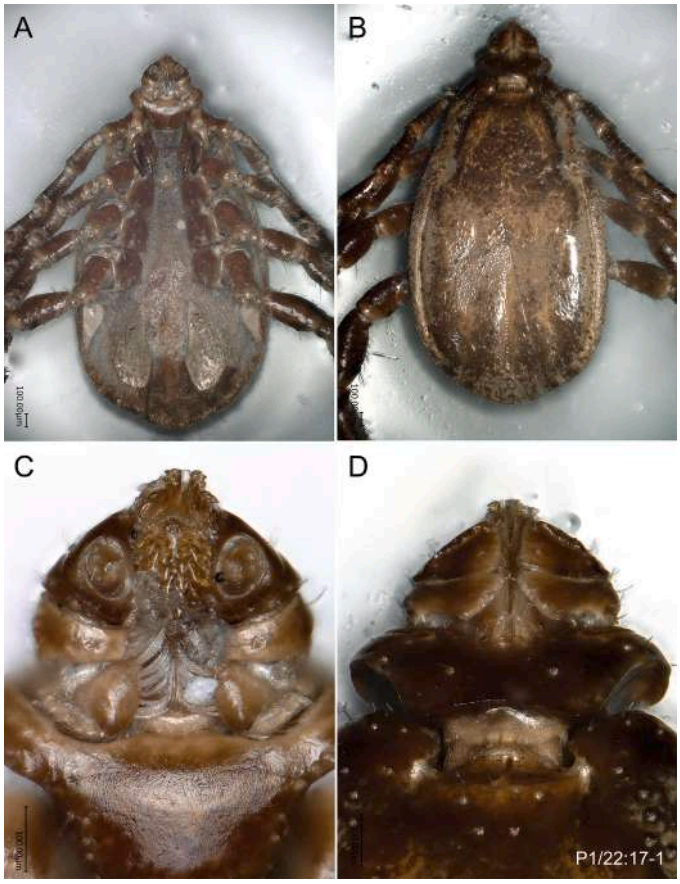

Fig. 1. Neotype *Rhipicephalus linnaei* (Audouin, 1826) unengorged adult male (P1/22:17-1) from Esna, Egypt. (A) Ventral side showing the subtriangular adanal shields and clearly visible festoons. Coxa I with two long triangular spurs. (B) Pear-shaped shape from the dorsal view with clearly visible flat eyes and scutum with deep, lateral grooves. (C) Basis capitula ventrally smooth with a mildly convex posterior margin, palpi short and stout. Palpi ventrally with a conspicuous subtriangular plate which bears on its inner margin curved, parallel, irregularly branched hairs. Hypostome short, blunt, dental formula 3/3, apex with well-developed corona of fine denticles. (D) Basis capituli dorsally hexagonal, wider than long, lateral angles prominent and pointed. Scale bar: 100 μm.

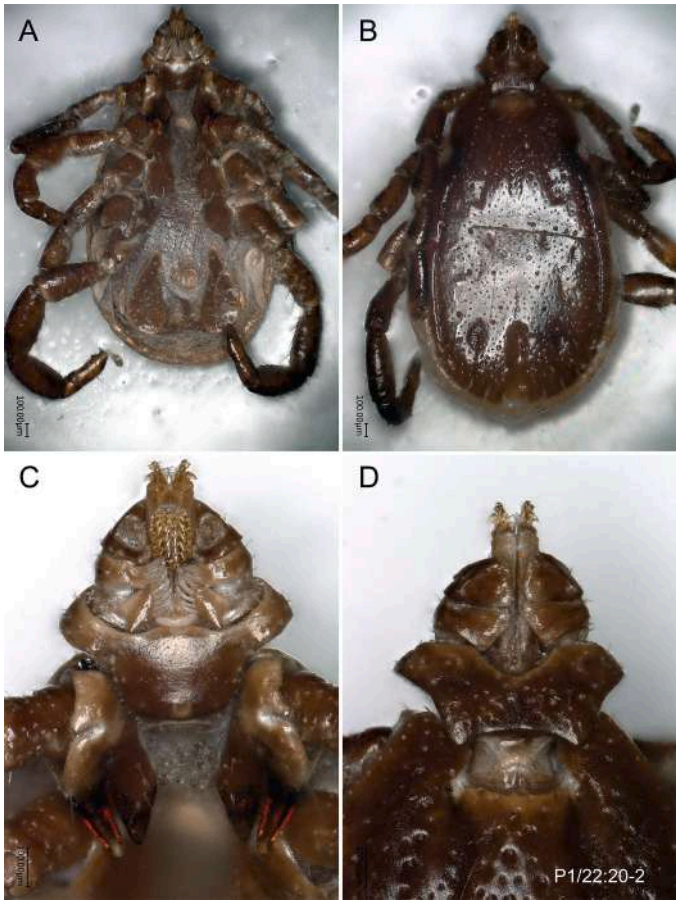

Fig. 2. *Rhipicephalus linnaei* (Audouin, 1826) unengorged adult male (P1/22:20-2) from Esna, Egypt. (A) Ventral side showing the subtriangular adanal shields and clearly visible festoons and the left elongated spiracular plate (B) Dark brown pear-shaped dorsal view with clearly visible flat eyes and scutum with deep, lateral grooves. Note the conspicuous large and small punctuation on the scutum. (C) Basis capitula ventrally smooth, palpi short and stout. Palpi ventrally with a conspicuous subtriangular plate. Hypostome short, blunt, dental formula 3/3, apex with well-developed corona of fine denticles. Coxa I with two long triangular spurs. (D) Basis capituli dorsally hexagonal, wider than long, lateral angles prominent and pointed. Scale bar: 100 μm.

obtained mitogenomes as well as all available mitogenomes from within *R. sanguineus* s.l. To reconstruct the amino acid alignments, all 13 individual genes were translated from each mitogenome to create 13 individual amino acid alignments that were then concatenated into final amino acid alignment from 18 mitogenomes. The phylogenetic tree was inferred by using the Maximum Likelihood (ML) method and mtREV24+G+F model as selected using a model selection process in MEGA 11. In addition, Minimum Evolution (ME) distance tree utilised evolutionary distances computed using the JTT+G model. The percentage of replicate trees in which the associated taxa clustered together was calculated for bootstrap test (200 replicates for ML, 500 replicates for ME) are shown above the branches. For distance tree reconstruction all ambiguous positions were removed for each sequence pair (pairwise deletion option). There were a total of 3,594 positions in the final dataset. The nucleotide mitogenome sequence alignment was used to extract the regions amplified by the PCR primers for *cox*1 gene, 12S rRNA gene and 16S rRNA gene. Each partial *cox*1, 12S rRNA gene and 16S rRNA gene alignment was used to infer phylogeny using the ME method. The percentage of replicate trees in which the associated taxa clustered together was used for a bootstrap test (1,000 replicates). The evolutionary distances were computed using the K2P+G model. All ambiguous positions were removed for each sequence pair (pairwise deletion option).

The *cox*1 gene phylogeny included all newly obtained sequences ($n = 21$) from Egypt as well as all *cox*1 sequences belonging to *R. sanguineus* s.l. "tropical lineage" available in GenBank. In addition, we included all available complete mitogenome *cox*1 sequences as well as *R. guilhoni* as the closest relative to *R. sanguineus* s.l. "tropical lineage". Two sequences from *R. microplus* and *R. australis* served as the outgroup. The alignment was constructed with the aid of amino acid sequences. The *cox*1 phylogenetic tree was based on nucleotide (nt) alignment was inferred by using the Maximum Likelihood method and Maximum Composite Likelihood approach with a discrete Gamma distribution among sites (+G) for *cox*1 alignment and ambiguous positions were removed for each sequence pair (pairwise deletion option). There was a total of 1539 positions in the final dataset. The percentage of replicate trees in which the associated taxa clustered together was calculated for bootstrap test (1,000 replicates).

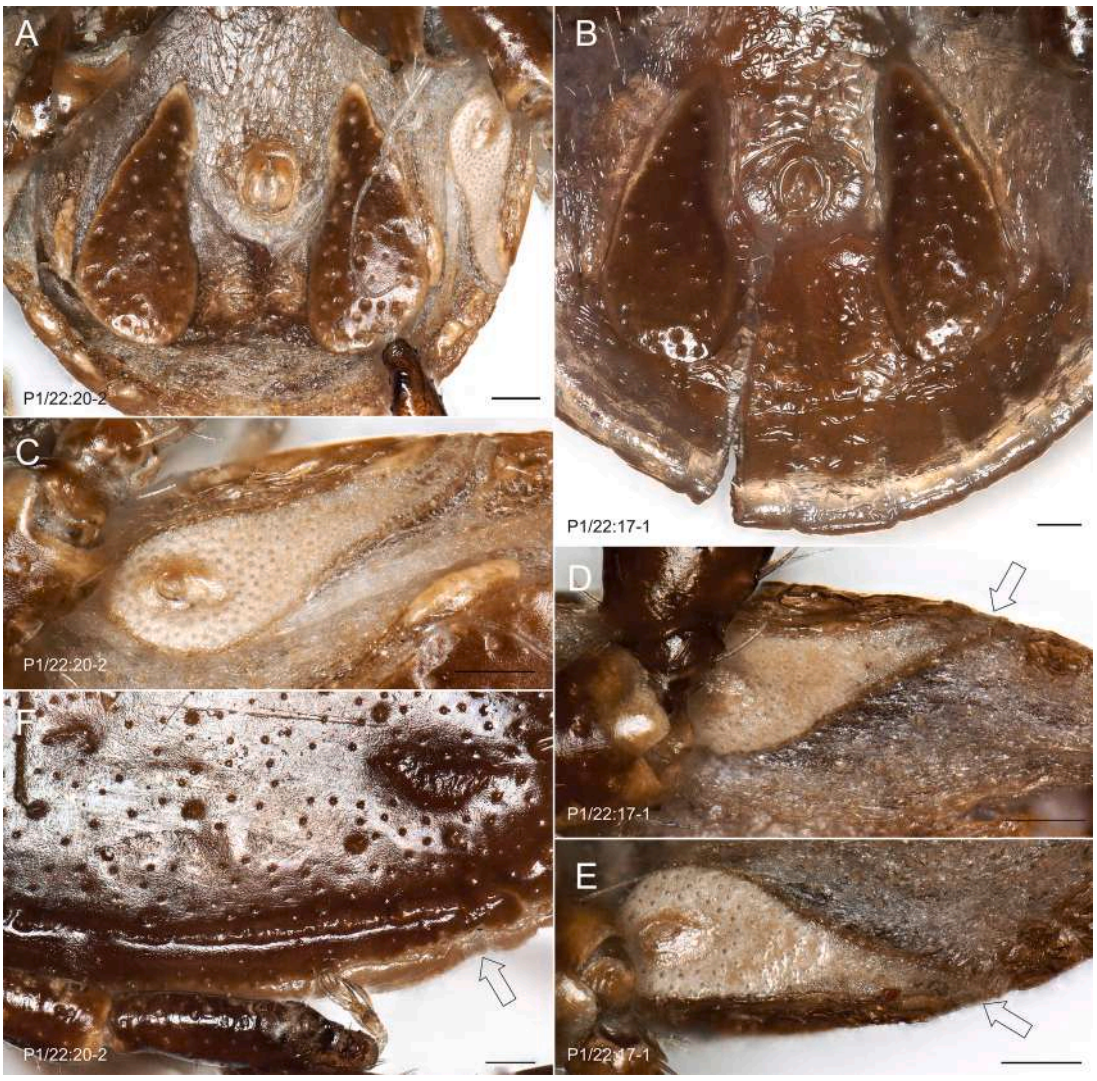

Fig. 3. *Rhipicephalus linnaei* (Audouin, 1826) unengorged adult male (P1/22:20-2 and P1/22:17-1) from Esna, Egypt. (A, B) Subtriangular shape of the adanal shields with the internal margin mildly concave anteriorly, its posterior usually rounded, not spur-like. (C, D, E) Spiracular plates narrowly elongate, comma-shaped, dorsal prolongation narrow and dorsal prolongation narrower than the width of adjacent festoon. (F) Dorsal prolongation of spiracular plate visible dorsally (arrow). (P1/22:20-2: A, C, F and P1/22:17-1: B, D, E). Scale bar: 100 μm.

3. Results

3.1. Neotype specimen and redescription

Rhipicephalus linnaei (Audouin, 1826)

Ixodes linnaei Audouin, 1826: Plate 9, Fig. 12.
Rhipicephalus linnei (*sic*).— Koch, 1844: 238.
Rhipicephalus sanguineus.— Hoogstraal, 1956: 686 (in part).
Rhipicephalus sanguineus.— Roberts, 1965: 492.
Rhipicephalus sanguineus.— Camicas et al., 1998: 161 (in part).
Rhipicephalus linnaei.— Šlapeta et al., 2021: 431.

Specimens examined

Neotype male and 20 additional vouchers (8 males, 7 unengorged females, 5 engorged females) were collected on dogs in Esna City, Luxor Governorate, Egypt (25°17′36.0″N 32°33′23.0″E; 25.293333, 32.556389), during the last week of October 2021, collected by Sobhy Abdel-Shafy. The neotype (P1/22:17-1) together with an adult female voucher (P1/22:6-1) is deposited in the Arachnid Collection of Egypt (ACE: ACE.2022.08.08.IXO.001 and ACE.2022.08.08.IXO.002), Heliopolis, Cairo, Egypt. The remaining vouchers are deposited in the Museum für Naturkunde, Berlin (ZMB: ZMB_Arach 50,630 to ZMB_Arach 50,633), Germany [males: P1/22:18-5, P1/22:19-1; females: P1/22:18-3, P1/22:18-4] and the Australian National Insect Collection (ANIC: ANIC 48 006 593 to ANIC 48 006 602), CSIRO, Canberra, Australian Capital Territory, Australia [males: P1/22:6-2, P1/22:10-1, P1/22:14-1, P1/22:20-1, P1/22:20-2, P1/22:21-1; females: P1/22:4-1, P1/22:12-1, P1/22:16-1, P1/22:18-1] (Tables S1 and S2).

Taxonomic notes

Rhipicephalus linnaei was described as *Ixodes linnaei* by Audouin (1826). Koch (1844) transferred it to the genus *Rhipicephalus* as a valid species separate from *R. sanguineus*. Since that time the status of *Ixodes linnaei* has remained unresolved and ambiguous (Šlapeta et al., 2021). Most general papers about *R. sanguineus sensu lato* include the populations that we now recognise as *R. linnaei*, either explicitly or implicitly. For that reason it is not possible to produce a comprehensive and detailed synonymy for the species, and we have listed only a few key papers.

Table 1
Morphological measurements of *Rhipicephalus linnaei* males.

Male	Mean (mm)	SD (mm)	Minimum (mm)	Maximum (mm)
Body (total length)	3.160	0.193	2.896	3.386
Body (exclusive of capitulum)	2.601	0.190	2.301	2.862
Body (maximum width)	1.779	0.182	1.556	2.088
Capitulum (width)	0.638	0.028	0.586	0.672
Capitulum (length, dorsal)	0.252	0.031	0.191	0.290
Palpal apices to cornua apices (length)	0.535	0.059	0.466	0.650
Palpi (length)	0.266	0.031	0.228	0.321
Dental formula	3/3	–	–	–
Hypostome (length)	0.269	0.019	0.250	0.295
Scutum (length)	2.623	0.189	2.253	2.908
Ventral shields (length)	0.727	0.060	0.658	0.828
Ventral shields (width)	0.308	0.038	0.225	0.360
Ventral shields (length to width ration)	2.38	0.29	2.16	2.95
Spiracular plate (length)	0.526	0.044	0.465	0.589
Spiracular plate (width)	0.179	0.019	0.157	0.208
Spiracular plate (width of dorsal end)	0.041	0.005	0.0037	0.050
Tarsus I (length)	0.554	0.026	0.0509	0.593
Tarsus IV (length)	0.507	0.028	0.456	0.559

Note: Based on seven male specimens deposited in the tick collections of the Arachnid Collection of Egypt, Heliopolis, Cairo, Egypt; Museum für Naturkunde, Berlin, Germany; and the Australian National Insect Collection, CSIRO, Canberra, Australian Capital Territory, Australia.

Redescription

Male

Figs. 1–3 and Table 1

Diagnosis: festoons distinct, the median festoon usually protruding posteriorly; basis capitula sharply hexagonal; cornua strong. Palpal article I ventrally with a conspicuous subtriangular plate. Dentition 3/3. Scutum with deep, lateral grooves enclosing two festoons; posteromedian and paramedian grooves distinct and deep, the former elongate, the latter subcircular or broadly oval; punctations consisting of a number of fairly large, discrete, piliferous punctations arranged in four more or less regular rows and a variable number of small interstitial punctations. Adanal shields subtriangular, the internal margin mildly concave anteriorly, its posterior angle usually rounded, never spur-like. Spiracular plate narrowly elongate comma-shaped. Coxa I deeply cleft into two elongate subequal spurs. Tarsi II-IV strongly bicalcarate.

Body: outline pear-shaped or broadly oval, widest in region of legs IV and spiracular plate, slightly narrower anteriorly, with a small concave margin at level of eyes. Integument bulging both laterally and posteriorly as engorgement proceeds; unengorged body measurements (exclusive of capitulum) 2.3 × 1.6–3.4 × 2.1 mm (range min.–max.). Colour usually dark brown, but sometimes lighter.

Scutum: moderately convex, 2.3 × 1.6–2.9 × 2.1 mm (range min.–max.). Inornate, reddish-brown colouration. Punctations moderate in number, unequal in size, larger and more densely distributed in anterior field; numerous fairly large piliferous punctations, sometime arranged linearly on each side extending from the cervical pits to near the commencement of the lateral grooves, arrangement in four longitudinal rows. Finer, interstitial punctations vary in number and definition. Piliferous punctations along the lateral margins of the scutum. Marginal (lateral grooves) groove deep and punctate, delimiting the first two festoons, extending anteriorly to level between legs III and II (or little posterior to the eyes). Cervical grooves short, deep, comma-shaped. Posteromedian groove usually distinct, elongate; posterolateral grooves usually distinct sub-circular, shorter than posteromedian groove. Eyes flat and mildly convex. Scapulae rounded.

Festoons: quadrangular in shape, distinct, the median festoon only slightly swollen and only marginally protruding posteriorly, with very few setiferous punctations.

Ventral plates: adanal plates long, adanal shields subtriangular, about 2.2–3.0 times as long as wide, the external and posterior margins curved, the posterior external angle broadly rounded, inner margin concave anteriorly, the posterior angle never spur-like. Accessory adanal plates conspicuous and pointed posteriorly.

Spiracular plate: narrowly elongate, subtriangular in shape, comma-shaped, dorsal prolongation narrow and usually visible dorsally, dorsal prolongation narrower than the width of adjacent festoon, greatest dimension 0.5–0.6 mm.

Capitulum: basis capituli dorsally hexagonal, wider than long, width 0.59–0.67 mm, length 0.19–0.29 mm (dorsal view). Lateral angles prominent and pointed, posterior margin concave, with usually strong, blunt cornua. Basis ventrally smooth with a mildly convex posterior margin. Palpi short and stout, 0.23–0.32 mm in length; articles 2 and 3 subequal, article 1 seen dorsally as a small sharp point on the inner side and ventrally with a conspicuous subtriangular plate which bears on its inner margin 6–8 long, curved, parallel, irregularly branched hairs; ventrally, article 2 with 5–6 similar hairs internally, and article 3 with 3–4 simple hairs. Hypostome short, blunt, dental formula 3/3 in 7–8 rows, apex with well-developed corona of fine denticles.

Legs: moderate length and becoming stronger posteriorly. Coxa I with two long, subequal, closely set, pointed spurs, the inner broader than the outer. Coxae increasing in size from I to IV. Coxae II-IV each with a small, triangular external spur, very small on coxa IV. Tarsi tapering gently; tarsus I without ventral spurs; tarsi II-IV each with strong terminal and subterminal ventral spurs.

Genital aperture: at level of anterior portion of coxa II.

‖

Female

Figs. 4 and 5 and Table 2

Diagnosis: basis capituli resembles those in male with posterolateral angles not as prominent; porose areas moderate in size, usually oval. Palpi as in male. Dentition 3/3. Scutum almost as wide as long, only slightly longer, posterolateral margins obtusely angled, posterior angle with a small marginal expansion; cervical grooves long and delimited externally by lateral grooves; punctations numerous, the large punctations piliferous and scattered somewhat indiscriminately, the smaller punctations more numerous and more regularly distributed. Genital aperture broadly U-shaped. Coxa I as in male. Spiracular plate broad comma-shaped.

Body: unengorged specimens oval, broadest at level of insertion of legs IV, slightly narrower anteriorly, unengorged body measurements (exclusive of capitulum) 2.2 × 1.6–3.9 × 2.8 mm (range min.–max.). Colour usually dark brown, but sometimes lighter. Marginal grooves deep; posterior median and paramedian grooves well developed, narrow, elongate. Colour usually dark brown.

Scutum: inornate, yellowish- or reddish-brown colouration, barely longer than broad, posterior margin sinuous obtusely angled, a little posterior to its mid-length, 1.0 × 1.0–1.4 × 1.3 mm (range min.-max.), length to width ratio 1.02–1.12, wides at the level of eyes. Eyes large, oval, and mildly convex. Lateral grooves deep well defined with large punctations and extending from commencement of cervical grooves to the scutal margin with the lateral ridge usually rounded. Cervical grooves short, deep converging anteriorly, shallow, and divergent posteriorly and forming with the lateral grooves an elongate, bow-shaped depression. Punctations moderate to numerous in number, unequal in size, the larger punctations piliferous, scattered or grouped in scapular and cervical areas, the smaller punctations abundant, appearing evenly distributed. Scapulae long, rounded. Alloscutum with three vertical linear grooves (inconspicuous in engorged females) and covered with scattered whitish and short setae.

Festoons: well defined in unengorged specimens, not visible in engorged specimens.

Spiracular plate: broadly comma-shaped, with narrow dorsal

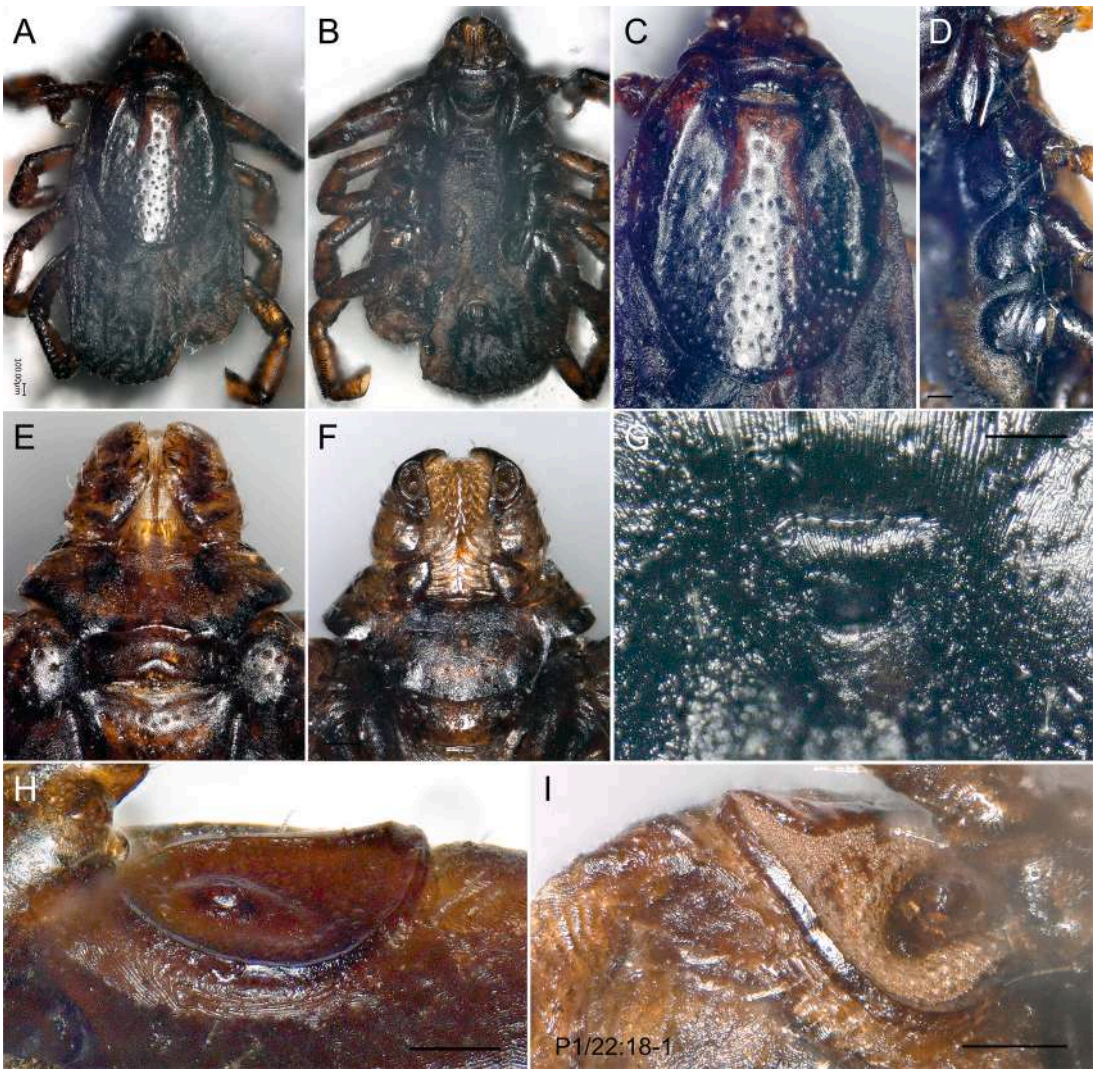

Fig. 4. *Rhipicephalus linnaei* (Audouin, 1826) unengorged female (P1/22:18-1) from Esna, Egypt. (A, B) Unengorged specimen oval, broadest at level of insertion of legs IV, slightly narrower anteriorly. (C) Scutum inornate, brown colouration, posterior margin sinuous obtusely angled, widest at the level of eyes. Lateral grooves deep well defined with large punctations. Cervical grooves with the lateral grooves form bow-shaped depression. Larger punctations more abundant anteriorly, while smaller punctuations appearing evenly distributed. (D) Coxa I with two long triangular spurs and coxae II-IV with a short triangular external spur and rounder internal spur. (E) Basis capituli dorsally hexagonal, wider than long and lateral angles prominent. Palpi short and rounded apically. (F) Basis capituli ventrally. Hypostome short, blunt. (G) Broad U-shape (cup-shaped) of the genital aperture that is widely open and rounded, wider than long. (H, I) Spiracular plates broad comma-shaped with narrow dorsal prolongation. Scale bar: 100 μm.

prolongation visible dorsally; greatest dimension about 0.4 mm. Goblets larger near the spiracular opening and very small and tight in the dorsal part of the spiracular plate.

Capitulum: basis capituli dorsally hexagonal, wider than long, width 0.55–0.66 mm, length 0.24–0.32 mm (dorsal view). Lateral angles prominent and pointed, posterior margin mildly concave with less developed cornua. Porose areas deep, oval and moderate in size, the interval more than the width of one but less than three times, depressed and with some punctuation. Palpi short and rounded apically as in males, in length 0.25–0.36 mm. Hypostome short, blunt, dental formula 3/3 in 7–8 rows, apex with corona of fine denticles.

Legs: coxa I with two long triangular spurs as in males, subparallel, the external narrower than the internal; coxae II-IV with a short triangular external spur and more round internal spur. In general female legs slender compared to males.

Genital aperture: sclerites of the aperture are transparent and the atrium of the genital pore is broadly U-shape (cup-shaped) located between coxae II in unengorged females, lateral margins of the atrium diverging laterally.

3.2. Differential diagnosis

Rhipicephalus linnaei is most similar to *Rhipicephalus sanguineus* (Latreille, 1806), *Rhipicephalus camicasi* Morel, Mouchet & Rodhain, 1976 and *R. leporis* Pomerantsev, 1946, because only these species share elongated long comma-like spiracula that are narrow and usually visible dorsally and the dorsal prolongation is narrower than the width of adjacent festoon. The male of *R. camicasi* is distinguished from *R. linnaei* by the non-tapering caudal widening of the spiracula. The sclerites of the female genital aperture are transparent in *R. linnaei* and the atrium of the genital pore is a wide U-shape, which means that it rather evokes *R. camicasi* and *R. sanguineus*. Similarly, *R. leporis* Pomerantsev, 1946 based on the original illustration closely resembles *R. linnaei* including the shape of the spiracula, that in a male are, however, more constricted at the dorsal prolongation. The male of *R. sanguineus* sensu stricto is distinguished from *R. linnaei* by shorter extension that does not taper into a long narrow extension of the spiracula. The female genital pore is a narrower U-shape in *R. sanguineus* sensu stricto compared with *R. linnaei*. In addition, *R. linnaei* are generally smaller than *R. sanguineus*

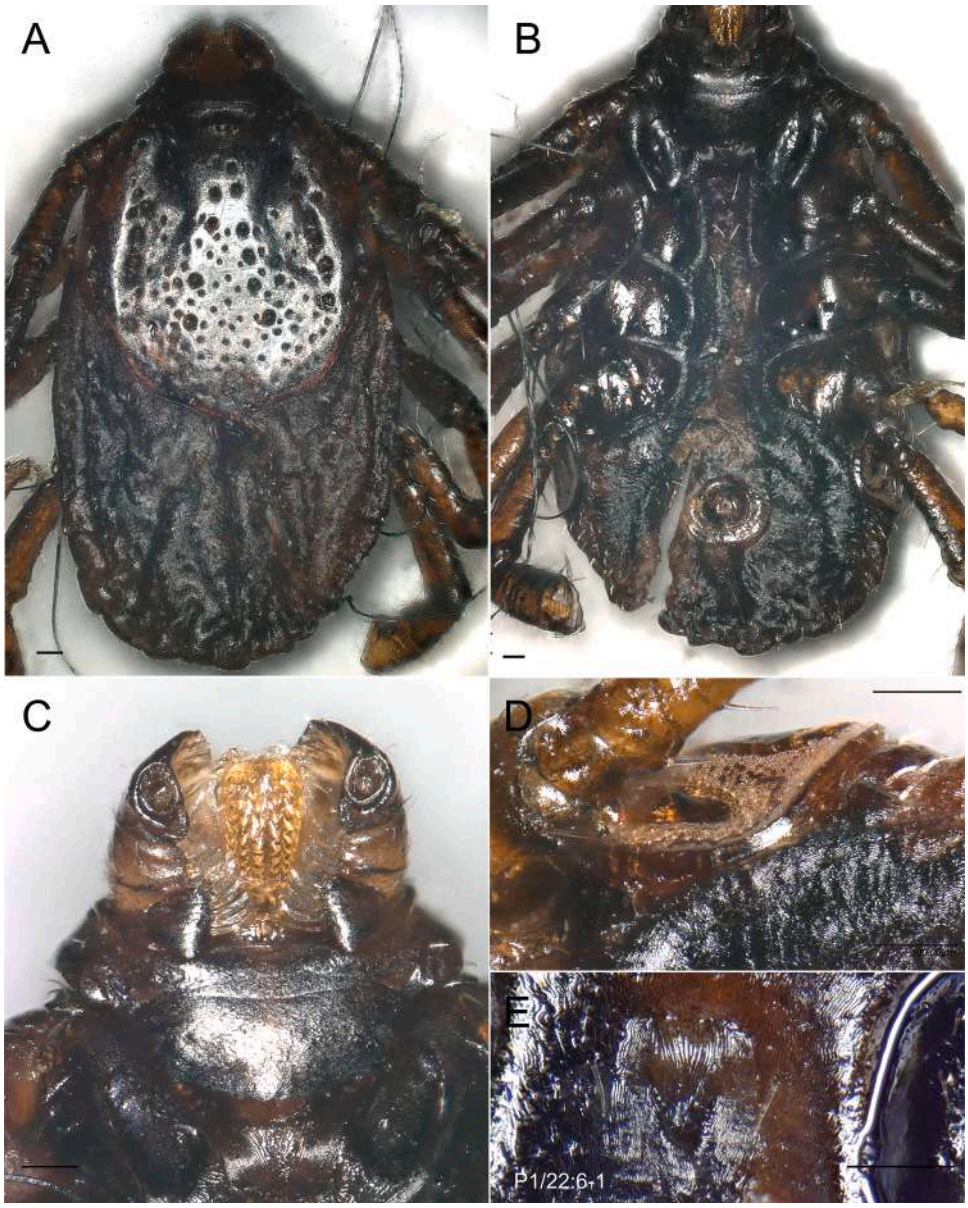

Fig. 5. *Rhipicephalus linnaei* (Audouin, 1826) unengorged female (P1/22:6-1) from Esna, Egypt. (A) Unengorged specimen oval, scutum inornate, brown colouration, posterior margin sinuous obtusely angled, widest at the level of eyes. Cervical grooves with the lateral grooves form bow-shaped depression. Larger punctations more abundant anteriorly, while smaller punctuations appearing evenly distributed. (B) Coxa I with two long triangular spurs and coxae II-IV with a short triangular external spur and rounder internal spur. (C) Basis capituli ventrally. Hypostome short, blunt with 3/3 dental formula. (D) Spiracular plate broad comma-shaped with narrow dorsal prolongation. (E) The genital aperture view is obscured and distorted in this specimen, the view presented is from the side, thus not clearly showing the broad U-shape cup. Scale bar: 100 μm.

s.s. The remaining species – *Rhipicephalus sulcatus* Neumann, 1908, *Rhipicephalus turanicus* Pomerantsev, 1940, *Rhipicephalus guilhoni* Morel & Vassilades, 1963, *Rhipicephalus secundus* Feldman-Muhsam, 1952 and *Rhipicephalus afranicus* Bakkes, 2020 - within the *R. sanguineus* species complex, all exhibit broader dorsal prolongation of the spiracular plates with the dorsal prolongation as wide as adjacent festoon. The DNA sequence of *Rhipicephalus linnaei* is the most closely related to *R. guilhoni*. Using mitochondrial DNA sequences, *Rhipicephalus linnaei* forms a distinct phylogenetic lineage within the sequences belonging to the *R. sanguineus* species complex.

3.3. Molecular characterisation of Rhipicephalus linnaei from Egypt

Four tick vouchers (three males and one female) including the neotype (P1/22:17-1) of *R. linnaei* were subject to whole genome sequencing from which the complete mitogenome (mtDNA) was assembled. The four assembled mitogenome (14,711–14,716 kb) sequences of *R. linnaei* are >96.5% identical to each other (7–512 differences, Fig. 6). The newly obtained mitogenomes of *R. linnaei* are closely related (>96.5% nucleotide identity) to mitogenomes of *R. linnaei* from brown dog ticks from Australia, Laos, Fiji, and China. The mitogenome of the neotype (P1/22:17-1) of *R. linnaei* is 98.0–98.2% identical to *R. linnaei* from Australia, Laos, and Fiji (MW429381–MW429383; Šlapeta et al., 2021; previously recognised as *R. sanguineus* s.l. "tropical lineage" and *R. sanguineus* sensu Roberts, 1965) with 12–299 nucleotide differences. The mitogenome of the neotype (P1/22:17-1) of *R. linnaei* is 88.4% identical to *R. sanguineus* s.s. from the US (AF081829; Black and Roehrdanz, 1998) with 1718 nucleotide differences, and 92.0% identical to *R. camicasi* from Saudi Arabia (MZ323229; Chandra et al., 2019, 2022) with 1182 nucleotide differences. Using only protein coding sequences (12) translated into amino acids, the neotype (P1/22:17-1) of *R. linnaei* is 98.9–99.2%, 93.7% and 95.2% identical to *R. linnaei* from Australia, Laos, Fiji and China, *R. sanguineus* s.s. and *R. camicasi*, respectively.

Comparison of the available mitogenomes from *R. linnaei* showed that all (including the neotype) but one have high percent identity at both the nucleotide (>98.0%) as well as amino acid (>98.9%) level. The single outlier (P1/22:17-1) has at maximum 0.04 nucleotide distance and 0.02 amino acid distance from the remaining *R. linnaei* mitogenomes. Phylogenetic analysis based on amino acid sequence confirmed

Table 2
Morphological measurements of unengorged *Rhipicephalus linnaei* females.

Female	Mean (mm)	SD (mm)	Minimum (mm)	Maximum (mm)
Body (total length)	3.466	0.671	2.940	4.562
Body (exclusive of capitulum, unengorged)	2.890	0.642	2.264	3.849
Body (maximum width)	2.037	0.464	1.590	2.813
Scutum (length)	1.246	0.141	0.972	1.444
Scutum (maximum width)	1163	0.111	0.953	1.293
Scutum (length to width ratio)	1.07	0.04	1.02	1.12
Capituli (width)	0.727	0.036	0.685	0.779
Basis (dorsal width)	0.582	0.036	0.550	0.658
Basis capituli (dorsal length)	0.272	0.022	0.244	0.315
Palpal apices to cornua apices (length)	0.644	0.057	0.550	0.710
Palpi (length)	0.312	0.046	0.245	0.363
Dental formula	3/3	–	–	–
Hypostome (length)	0.301	0.042	0.251	0.354
Spiracular plate (length)	0.399	0.056	0.337	0.460
Spiracular plate (width)	0.282	0.062	0.226	0.353
Spiracular plate (width of dorsal end)	0.053	0.010	0.045	0.068
Tarsus I (length)	0.575	0.052	0.502	0.642
Tarsus IV (length)	0.542	0.064	0.469	0.634

Note: Based on seven female specimens deposited in the tick collections of the Arachnid Collection of Egypt, Heliopolis, Cairo, Egypt; Museum für Naturkunde, Berlin, Germany; and the Australian National Insect Collection, CSIRO, Canberra, Australian Capital Territory, Australia.

the mitogenome (*R. linnaei*, P1/22:17-1) formed a sister lineage to the rest of the mitogenomes of *R. linnaei* (Fig. 7A). The closest sister species to *R. linnaei* mitogenomes are those from *R. camicasi*, maximum 0.08 nucleotide distance and 0.06 amino acid distance. The phylogenetic analysis resolved robustly with high (ML: 100%, ME: 100%) bootstrap support the monophyly of all the mitogenomes of *R. linnaei* from Egypt together with those from Australia, Laos, Fiji, and China (Fig. 7A).

We then used the complete mitogenome alignment to investigate the resolution using conventional PCR amplified mtDNA fragments including *cox*1, 12S rRNA gene and 16S rRNA gene (Fig. 7B). Phylogenetic analysis of all three fragments robustly resolved the monophyly of sequences belonging to *R. linnaei* (>94% bootstrap support). The branching order of the sequences belonging to *R. sanguineus* s.l., however, was weakly supported or differed to that resolved using whole mitogenomes. While 12S rRNA gene and *cox*1 gene partial sequences resolved correct branching order for *R. camicasi* and *R. sanguineus* "southeastern Europe" lineage, the support values were low. The 16S rRNA gene tree resolved different branding order for *R. camicasi* and *R. sanguineus* "southeastern Europe" lineage with low support values, including <50% for *R. camicasi* 16S rRNA gene sequences (Fig. 7B). The placement of *R. sanguineus* s.s., *R. turanicus* and *R. secundus* was weakly supported in all three single gene phylogenies.

3.4. *Rhipicephalus linnaei and Rhipicephalus turanicus from Egypt*

During the quest for the neotype of *R. linnaei* in Esna City, Luxor Governorate, Egypt in total 34 ticks were collected from 21 dogs (P1/22:1 to P1/22:21). All ticks collected belonged to *R. sanguineus* s.l. For 26 ticks, we successfully amplified a fragment of the *cox*1 gene using PCR. Sequence comparison confirmed 21 sequences had high sequence identity to *R. linnaei* and five to *R. turanicus* (Supplementary Table S1). Phylogenetic analysis of the partial *cox*1 gene focused on the publicly available *cox*1 partial sequences from Africa specifically those belonging to *R. linnaei* (Fig. 8). In addition, *R. guilhoni cox*1 gene sequences were included because of close phylogenetic relationship with *R. linnaei* and those *cox*1 gene sequences annotated "*R. leporis*". Phylogenetic analysis showed monophyly of all *R. linnaei* sequences from Egypt with those from Africa as well as those recognised in GenBank as "*R. leporis*" that likely represent misidentification (Fig. 8). Similarly, selection of available *cox*1 sequences from ticks from all continents apart of Antarctica belong to *R. linnaei* (inset in Fig. 8). The sequences of *R. guilhoni* formed a robust sister clade to the *R. linnaei* sequences (Fig. 8). Single sequence from *R. linnaei* (P1/22:20-2) was distinct from the remainder of newly obtained *R. linnaei* sequences (Fig. 8). Four of the *R. linnaei* were subject to whole genome sequencing including vouchers from single dog (P1/22:20-1 and P1/22:20-2) described above. To verify the *cox*1 PCR amplification for P1/22:20-2, we repeated it using an alternative set of primers and confirmed to be 100% identical. All PCR amplified *cox*1 gene sequences were 100% identical to *cox*1 for their respective assembled mitogenomes from whole genome sequence data. The *cox*1 sequences belonging to *R. turanicus* were phylogenetically resolved as closely related to the reference *R. turanicus* (NC_035946) (Fig. 8). To complement *cox*1 gene sequence data from *R. turanicus*, we obtained additional 16S rRNA gene and 12S rRNA gene sequence data for two ticks that showed close identity to the reference *R. turanicus* (NC_035946). Dog P1/22:16 was coinfested with *R. linnaei* and *R. turanicus*.

Using molecular identification and in particular *cox*1 close sequence identity, *R. linnaei* is globally distributed across Africa, Australia, Asia, South and North Americas as well as southern Europe (Fig. 8., see also Šlapeta et al., 2021).

4. Discussion

This study re-established the name *Rhipicephalus linnaei* for the species now represented by a neotype collected from Egypt, the type locality of the lost original type material (Audouin, 1826). A male tick was selected as the neotype to match the sex of the originally illustrated specimen on "Planche 9″ (https://doi.org/10.11588/diglit.4742#0051), where the tick illustration is Fig. 12 (Audouin, 1826). The species is morphologically redescribed using a series of vouchers collected from dogs from which the neotype was selected. To substantiate and enrich the description, we have obtained genetic sequences from the series as well as whole genome sequences that enabled us to assemble whole mitogenome of the neotype to serve as genetic reference for the species. Importantly, the reproductive isolation between *R. linnaei* (=*R. sanguineus* s.l. "tropical lineage") and *R. sanguineus* s.s. was established using colony ticks from Brazil and Argentina, respectively (Szabó et al., 2005; Nava et al., 2018).

The neotype has been established in accordance with the Article 75 (ICZN, 1999). Initially, Šlapeta et al. (2021) believed that the Australian *R. sanguineus* described by Roberts (1965) and later associated with the "tropical lineage" of *R. sanguineus* by Chandra et al. (2022), is genetically compatible with the lost type material of *Ixodes linnaei* (=*Rhipicephalus linnaei*) from Egypt because *R. sanguineus* "tropical lineage" has also been found in Egypt by Chitimia-Dobler et al. (2017). This initial suggestion has been challenged as untenable without explicit redescription using material from the type locality (Guglielmone et al., 2015 and updates; Chitimia-Dobler et al., 2017; authors' communications; Mumcuoglu et al., 2022). The present primary purpose is to clarify the taxonomic status of the taxon (Article 75.3.1). The morphological and genetic description presented enables differentiating the taxon for which the neotype was designated from other taxa and describes the means to recognise it (Article 75.3.2 and Article 75.3.3). The original name-baering type is lost or destroyed, in telling analogy with the lost name-bearing type for *Haemaphysalis leachii* (Audouin, 1826), collected and described from Egypt by Jean Victor Audouin in "*Explication Sommaire des Planches d'Arachnides de l'Égypte et de la Syrie*" (Hoogstraal, 1958, cited as Professor M. Andre, correspondence) (Article 75.3.4). The neotype was collected from the type locality and is consistent with what is known of the former name-bearing type (Article 75.3.5 and Article 75.3.6). The neotype is deposited and becomes the public property of the Arachnid Collection of Egypt, Heliopolis, Cairo,

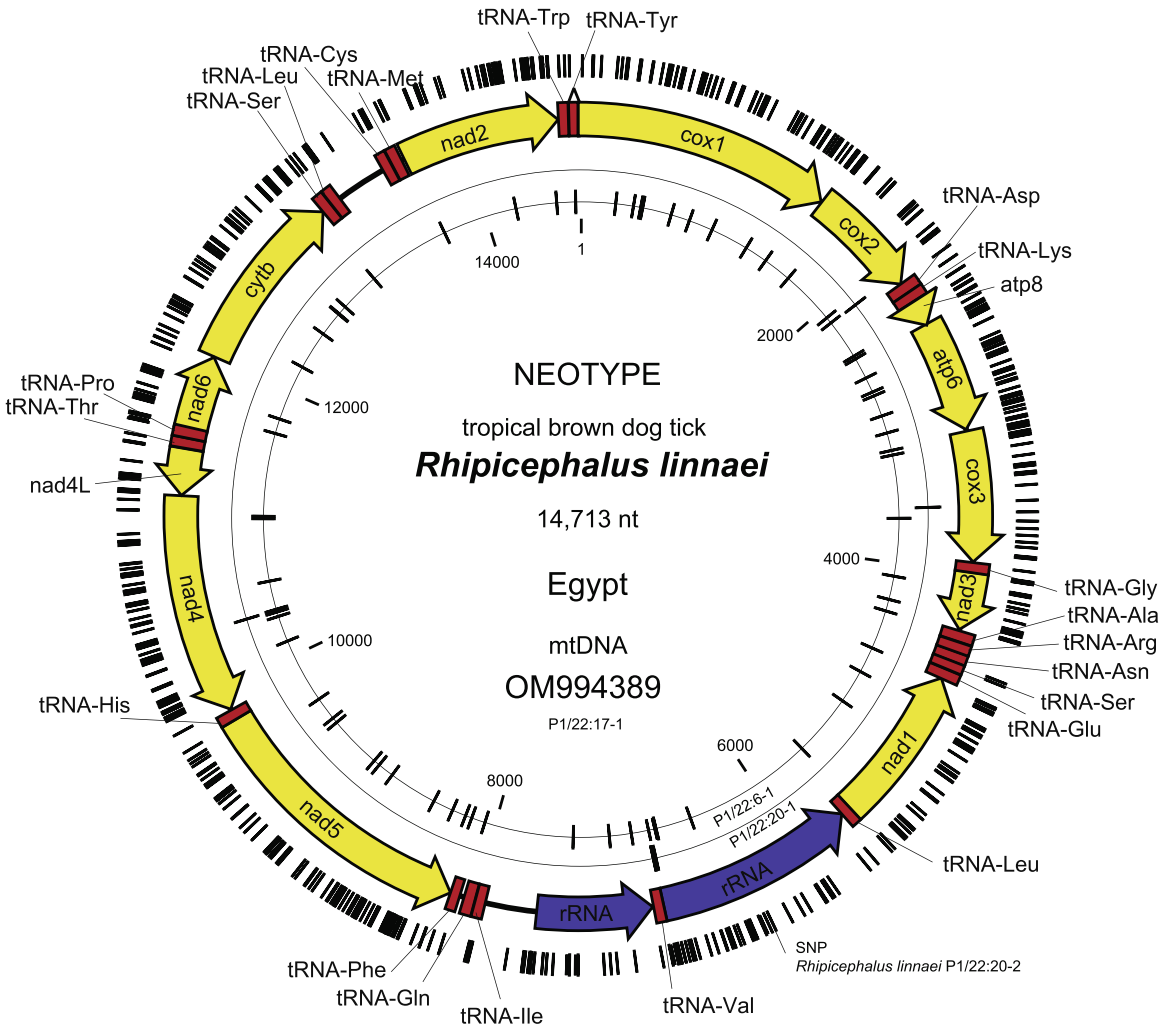

Fig. 6. Neotype of *Rhipicephalus linnaei* mitochondrial genome organisation. The mitogenome (mtDNA) from neotype from Esna, Egypt collected from domestic dog. The circular genome includes 13 protein coding genes (yellow), two rRNA genes (blue) and 22 tRNAs (red). The inner and outer circles represent mtDNA obtained from other *R. linnaei* ticks from the same locality with black lines representing single nucleotide polymorphisms (SNPs), differentiating it from the neotype mtDNA.

Egypt (Article 75.3.7).

Morphologically and genetically characterised Australian and Egyptian specimens of *R. sanguineus* s.l. "tropical lineage" previously described from Australia (Chandra et al., 2020, 2021) and by Chitimia-Dobler et al. (2017) from Egypt represent *R. linnaei* as previously proposed by Šlapeta et al. (2021). There is no need to establish a new name for the Australian and/or South East Asian brown dog tick, because that name would be a junior synonym of *R. linnaei*. The detailed description of adults, nymphs, and larvae of *R. sanguineus* sensu Roberts (1965), represents descriptions of *R. linnaei* because unlike in Egypt, there is only *R. linnaei* from the *R. sanguineus* species complex in Australia (Roberts, 1965; Barker and Walker, 2014; Barker et al., 2014; Chandra et al., 2020, 2021; Šlapeta et al., 2021). Morphological descriptions of *R. sanguineus* s.l. that could represent *R. linnaei* from Africa have to be taken with caution due to existence of possible cryptic species (i.e., Hoogstraal, 1956; Morel and Vassiliades, 1962; Hafez, 1981).

Morphological identification of individual species within the brown dog species complex (*R. sanguineus* s.l.) in Africa, Mediterranean, southeastern Europe and Middle East is difficult (Ondrejicka et al., 2014; Hekimoglu et al., 2016; Chitimia-Dobler et al., 2017; Hornok et al., 2017; Nava et al., 2018; Bakkes et al., 2020; Coimbra-Dores et al., 2020; Mumcuoglu et al., 2022). While morphological identification is challenging, molecular tools using short mtDNA regions such as 12S rRNA, 16S rRNA and *cox*1 genes are now routinely used for *R. sanguineus* s.l. specimens. The use of short sequences can serve for species identification assuming the database is sufficiently rich. We demonstrated here the drawback with short sequence data leading to unresolved phylogeny for which the whole mtDNA sequence was far superior. Consequently, molecular approaches come with a new set of challenges. Ideally there should be census of available species to undertake DNA barcoding that would establish criteria for maximum within species and minimum between species distances (Besansky et al., 2003; Hajibabaei et al., 2007; Hansen et al., 2007; Ondrejicka et al., 2014). However, initial research on the taxon formally considered as *R. sanguineus* recognised it as probable composite species in other words a candidate for taxonomical split. The supposed DNA barcoding approach has been presented with description of *R. afranicus* (Bakkes et al., 2020). The authors started with morphologically described vouchers for which they obtained molecular barcodes but did not define DNA barcoding criteria for maximum within species and minimum between species distances (Bakkes et al., 2020). Most other published works present what is rather called DNA taxonomy, with arbitrary assigning of taxa to phylogenetic clades (Moraes-Filho et al., 2011; Liu et al., 2013; Hekimoglu et al., 2016; Chitimia-Dobler et al., 2017; Hornok et al., 2017; Ravi et al., 2019; Coimbra-Dores et al., 2020; Alghamdi et al., 2021; Kamani, 2021; Elelu et al., 2022). The major two challenges remain: (i) absence of robust reference sequences associated with morphological vouchers and (ii) absence of criteria such as the maximum within species and minimum

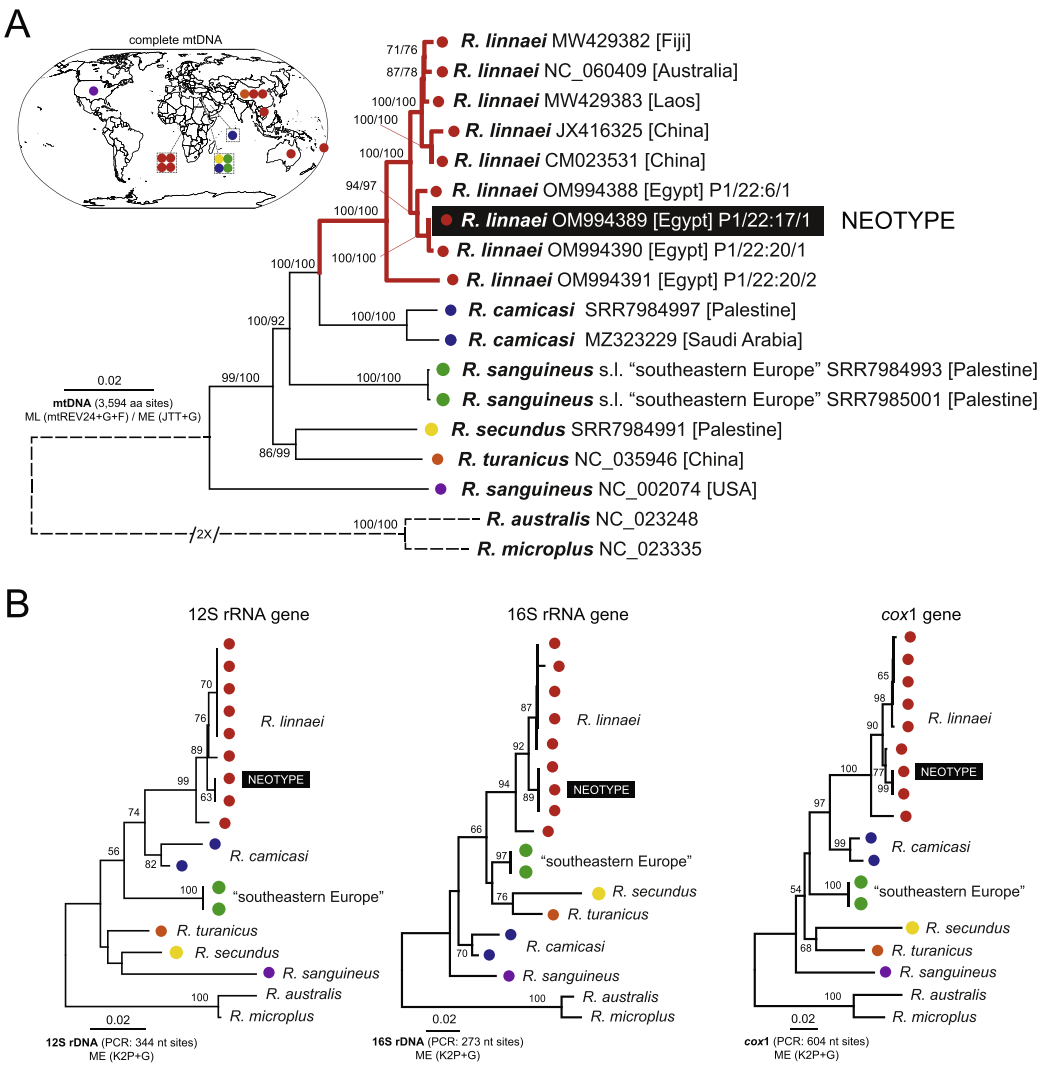

Fig. 7. *Rhipicephalus sanguineus* sensu lato (s.l.) mitogenome phylogeny. (A) The mitochondrial genomes (mtDNA) for *Rhipicephalus linnaei* from Esna, Egypt with all available mitogenomes for *R. sanguineus, R. linnaei, Rhipicephalus turanicus, Rhipicephalus camicasi, Rhipicephalus secundus* and *R. sanguineus* s.l. "southeastern Europe" were included and aligned. The complete mtDNA were assembled de novo from FastQ reads as describe in Šlapeta et al. (2021) belonging to *R. secundus* (SRR7984991) from Palestine: Nablus (tick_13, NST3.1, sheep), *R. camicasi* (SRR7984997) from Palestine: Tubas (tick_8, TDT3.1, dog) and two *R. sanguineus* s.l. "southeastern Europe" (SRR7984993, SRR7985001) from Palestine: Hebron (tick_10, NST2.1, sheep) and Nablus (tick_12, HDT1.1, dog) (Ravi et al., 2019). The mtDNA phylogenetic tree based on amino acid data from all 13 coding genes was inferred by using the ML method and General Reversible Mitochondrial + Freq. (mtREV24 + F) model with a discrete Gamma distribution among sites (+G). Map and colour coded markers indicate the location of the tick on the world map. The percentage of trees in which the associated taxa clustered together is shown below the branches (as the percentage from 200 replicates) using ML method and distance method (Minimum Evolution: JTT+G model). (B) Phylogenetic relationship of partial 12S rRNA, 16S rRNA and *cox*1 genes extracted from the complete mtDNA alignment based on traditionally PCR amplified regions. The phylogenetic trees were inferred using the Minimum Evolution method with Kimura-2 parameter (K2P) model with the rate variation among sites modelled with a gamma distribution (+G). The percentage of replicate trees in which the associated taxa clustered together in the bootstrap test (1,000 replicates) are shown next to the branches. All ambiguous positions were removed for each sequence pair (pairwise deletion option). All trees are rooted using *Rhipicephalus australis* and *Rhipicephalus microplus* sequences. Trees are drawn to scale, with branch lengths measured in the number of substitutions per site.

between species distances. Once the above is solidified an opportunity emerges to use geometric morphometrics to start to resolve the *R. sanguineus* complex (Bakkes et al., 2020). To address the first challenge, whole genome sequence data should be made available with deposited vouchers accessioned in reputable museums. To address the second challenge, the first challenge should be repeated for as many regions as possible to enable establishment of such distances for key markers that then could be used for DNA barcoding. Verified vouchers exist and were described and DNA methods were used for *R. sulcatus* Neumann, 1908, *R. turanicus* Pomerantsev, 1940, *R. guilhoni* Morel & Vassilades, 1963, *R. secundus* Feldman-Muhsam, 1952 and *R. afranicus* Bakkes, 2020 and so should be used for establishing such reference whole genome sequences (Nava et al., 2018; Bakkes et al., 2020; Mumcuoglu et al., 2022). Similarly, additional whole genome sequence data from the tick colony neotype material for *R. sanguineus* sensu stricto was selected and should be sequenced and made available for mitogenome assembly (Black and Roehrdanz, 1998; Nava et al., 2018). The cost of generating 1Gb whole genome data is currently equivalent to the cost of Sanger-sequencing 4–5 PCR amplicons, therefore financially accessible to any laboratory that already uses PCR and Sanger-sequencing for molecular identification of *R. sanguineus* s.l. ticks. Whole genome sequencing utilising Illumina next generation sequencing (NGS) requires only 100 pg to 500 ng of template DNA that is readily available and used for routine conventional PCR (Smith et al., 2021; Chandra et al., 2022). In fact, whole genome sequencing is a cost effective and future proof approach to voucher identification, because new markers can be assembled from the NGS data. Deposition of the NGS data to public genomic data repositories should be mandatory for such projects to enable new assemblies and verification of the published assemblies.

In conclusion, the identity of *R. sanguineus* s.l. "tropical lineage" is clarified by designation of a neotype for *Rhipicephalus linnaei*. The name *Ixodes linnaei* is the oldest available synonym of *R. sanguineus*. All other names that represent what was known as "tropical lineage" in the synonymy of *R. sanguineus* are junior synonyms of *linnaei* (Šlapeta et al.,

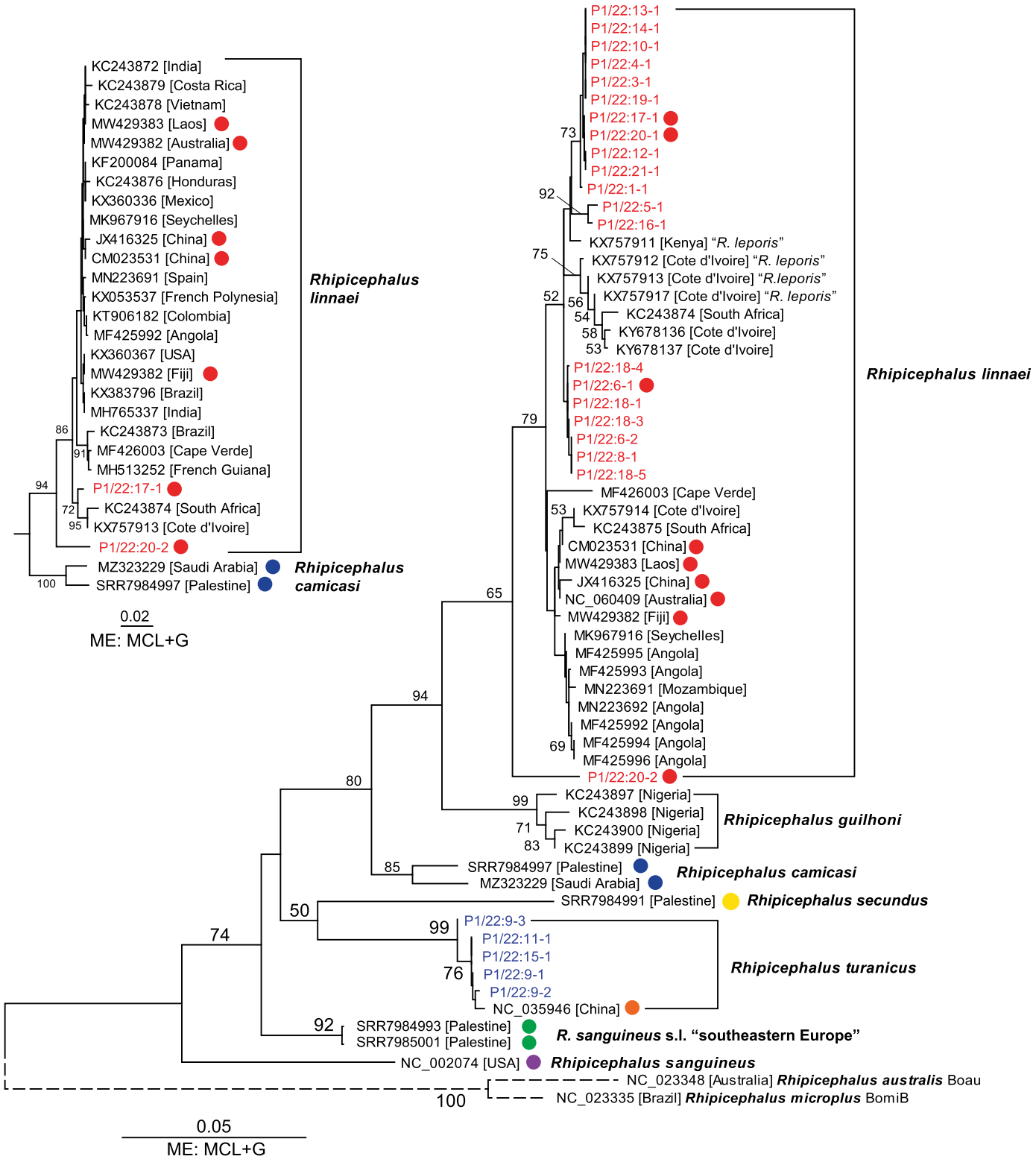

Fig. 8. Evolutionary relationships of *Rhipicephalus linnaei* and *Rhipicephalus turanicus* from Esna, Egypt based on partial mitochondrial DNA cytochrome c oxidase subunit I (*cox*1) gene. All available *cox*1 gene sequences from *R. linnaei* = *R. sanguineus* s.l. "tropical lineage" from Africa, *R. guilhoni* as well as complete mitogenomes (mtDNA) are included. The country of origin for each sequence is shown in square brackets. Mitogenomes are depicted by colourised circle. Newly obtained *cox*1 sequences of *R. linnaei* (red) and *R. turanicus* (blue) from dogs in Esna, Egypt are identified by their voucher number. An inset tree shows a phylogenetics tree with global selection of *cox*1 sequences belonging to *R. linnaei*, the tree was rooted with *R. camicasi cox*1 sequences. The evolutionary distances were computed using the Maximum Composite Likelihood method (MCL) method with the rate variation among sites modelled with a gamma distribution (+G). The percentage of replicate trees in which the associated taxa clustered together in the bootstrap test (1,000 replicates) are shown next to the branches. All ambiguous positions were removed for each sequence pair (pairwise deletion option). There were a total of 1,539 positions in the final dataset. The tree is rooted using *Rhipicephalus australis* and *Rhipicephalus microplus* sequences.

2021). To provide stability to the nomenclature, we have established the neotype and described the species using contemporary material and tools including morphology and comprehensive genetic characterisation. We place the species with the genus *Rhipicephalus*. The use of the name *R. linnaei* reduces the list of dubious names and is preferred to the introduction of a new potential synonym.

CRediT authorship contribution statement

Jan Šlapeta: Conceptualization, Methodology, Investigation, Resources, Data curation, Writing – original draft, Visualization, Project administration. **Bruce Halliday:** Conceptualization, Methodology, Investigation, Writing – review & editing. **Shona Chandra:** Methodology, Investigation, Writing – review & editing. **Abdullah D. Alanazi:** Resources, Writing – review & editing. **Sobhy Abdel-Shafy:** Methodology, Resources.

Data Availability

Raw FastQ sequence data were deposited at SRA NCBI BioProject: PRJNA812998. The nucleotide sequence data including four assembled mitogenomes generated in this study were deposited in GenBank (NCBI): OM994388-OM994391 (complete mtDNA), OM984968-OM984993 (*cox*1), OM984677-OM984681 (16S rRNA gene), OM984683-OM984684 (12S rRNA gene). All sequence data, associated supplementary material and additional data are available at LabArchives (https://dx.doi.org/10.25833/2h0k-n627).

Acknowledgments

We thank Hisham El-Hennawy from the Arachnid Collection of Egypt, Cairo, Egypt and Jason Dunlop from the Museum für Naturkunde, Berlin, Germany for arrangements with neotype and voucher deposition into museums. We thank Stephen Barker (University of Queensland) for extending an invitation to the Tick Mitochondrial Genome Network discussion #4 in late February 2021 that initiated the need to establish the neotype. We acknowledge the facilities, scientific and technical assistance with Artemis HPC provided by the Sydney Informatics Hub, Core Research Facilities of the University of Sydney.

Supplementary materials

Supplementary material associated with this article can be found, in the online version, at doi:10.1016/j.ttbdis.2022.102024.

References

Alghamdi, S.Q., Low, V.L., Alkathiry, H.A., Alagaili, A.N., McGarry, J.W., Makepeace, B. L., 2021. Automatic barcode gap discovery reveals diverse clades of *Rhipicephalus* spp. and *Haemaphysalis* spp. ticks from small mammals in 'Asir, Saudi Arabia. Parasite. Vectors 14, 541. https://doi.org/10.1186/s13071-021-05049-x.

Audouin, V., 1826. Explication Sommaire des Planches d'Arachnides de l'Égypte et de la Syrie. Description de l'Égypte ou Recueil des observations et des recherches qui ont été faites en Égypte pendant l'Expédition de l'armée française. 1st Edition. L'Imprimérie Impériale, Paris (Band 5,1,1: Texte 1: Histoire naturelle, p. 186; Band 5,2,1: Planches 1: Histoire naturelle, Pl. 9). doi:10.11588/diglit.472.

Bakkes, D.K., Chitimia-Dobler, L., Matloa, D., Oosthuysen, M., Mumcuoglu, K.Y., Mans, B.J., Matthee, C.A., 2020. Integrative taxonomy and species delimitation of *Rhipicephalus turanicus* (Acari: ixodida: ixodidae). Int. J. Parasitol. 50, 577–594. https://doi.org/10.1016/j.ijpara.2020.04.005.

Barker, S.C., Walker, A.R., 2014. Ticks of Australia. The species that infest domestic animals and humans. Zootaxa 3816, 1–144. https://doi.org/10.11646/zootaxa.3816.1.1.

Barker, S.C., Walker, A.R., Campelo, D., 2014. A list of the 70 species of Australian ticks; diagnostic guides to and species accounts of *Ixodes holocyclus* (paralysis tick), *Ixodes cornuatus* (southern paralysis tick) and *Rhipicephalus australis* (Australian cattle tick); and consideration of the place of Australia in the evolution of ticks with comments on four controversial ideas. Int. J. Parasitol. 44, 941–953. https://doi.org/10.1016/j.ijpara.2014.08.008.

Beati, L., Keirans, J.E., 2001. Analysis of the systematic relationahips among ticks of the genera *Rhipicephalus* and *Boophilus* (Acari: ixodidae) based on mitochondrial 12S ribosomal DNA gene sequences and morphological characters. J. Parasitol. 87, 32–48.doi:10.1645/0022–3395(2001)087[0032:AOTSRA]2.0.CO;2.

Bernt, M., Donath, A., Juhling, F., Externbrink, F., Florentz, C., Fritzsch, G., Putz, J., Middendorf, M., Stadler, P.F., 2013. MITOS: improved de novo metazoan mitochondrial genome annotation. Mol. Phylogenet. Evol. 69, 313–319. https://doi.org/10.1016/j.ympev.2012.08.023.

Besansky, N.J., Severson, D.W., Ferdig, M.T., 2003. DNA barcoding of parasites and invertebrate disease vectors: what you don't know can hurt you. Trends Parasitol. 19, 545–546. https://doi.org/10.1016/j.pt.2003.09.015.

Black, W.C., Roehrdanz, R.L., 1998. Mitochondrial gene order is not conserved in arthropods: prostriate and metastriate tick mitochondrial genomes. Mol. Biol. Evol. 15, 1772–1785. https://doi.org/10.1093/oxfordjournals.molbev.a025903.

Black, W.C.t., Piesman, J., 1994. Phylogeny of hard- and soft-tick taxa (Acari: ixodida) based on mitochondrial 16S rDNA sequences. Proc. Natl. Acad. Sci. U. S. A. 91, 10034–10038. https://doi.org/10.1073/pnas.91.21.10034.

Camicas, J.L., Hervy, J.P., Adam, F., Morel, P.C., 1998. Les Tiques du monde.(Acarida, Ixodida). Nomenclature, Stades décrits, Hôtes, Répartition. (Espèces décrites avant le 1/01/96) [The ticks of the world (Acarida, Ixodida): nomenclature, described stages, hosts, distribution. (Including new species described before 1/01/96)]. 233 p., Paris: Orstom Éditions. ISBN 2-7099-1418-2.

Chandra, S., Alanazi, A.D., Šlapeta, J., 2022. Mitochondrial genome of *Rhipicephalus* cf. *camicasi* Morel, Mouchet et Rodhain, 1976 from a camel (*Camelus dromedarius* Linnaeus) in Riyadh, Saudi Arabia. Folia Parasitol. 69, 005 https://doi.org/10.14411/fp.2022.005.

Chandra, S., Halliday, B., Šlapeta, J., 2021. Museum material of *Rhipicephalus sanguineus* sensu Roberts (1965) collected in 1902–1964 from Australia is identical to *R. sanguineus* sensu lato tropical lineage at the mitochondrial DNA 12S rRNA level. Med. Vet. Entomol. 35, 315–323. https://doi.org/10.1111/mve.12495.

Chandra, S., Ma, G.C., Burleigh, A., Brown, G., Norris, J.M., Ward, M.P., Emery, D., Šlapeta, J., 2020. The brown dog tick *Rhipicephalus sanguineus* sensu Roberts, 1965 across Australia: morphological and molecular identification of *R. sanguineus* s.l. tropical lineage. Ticks Tick Borne Dis. 11, 101305 https://doi.org/10.1016/j.ttbdis.2019.101305.

Chandra, S., Smith, K., Alanazi, A.D., Alyousif, M.S., Emery, D., Šlapeta, J., 2019. *Rhipicephalus sanguineus* sensu lato from dogs and dromedary camels in Riyadh, Saudi Arabia: low prevalence of vector-borne pathogens in dogs detected using multiplexed tandem PCR panel. Folia Parasitol. 66, 007 https://doi.org/10.14411/fp.2019.007.

Chitimia-Dobler, L., Langguth, J., Pfeffer, M., Kattner, S., Kupper, T., Friese, D., Dobler, G., Guglielmone, A.A., Nava, S., 2017. Genetic analysis of *Rhipicephalus sanguineus* sensu lato ticks parasites of dogs in Africa north of the Sahara based on mitochondrial DNA sequences. Vet. Parasitol. 239, 1–6. https://doi.org/10.1016/j.vetpar.2017.04.012.

Coimbra-Dores, M.J., Jaarsma, R.I., Carmo, A.O., Maia-Silva, M., Fonville, M., da Costa, D.F.F., Brandao, R.M.L., Azevedo, F., Casero, M., Oliveira, A.C., Afonso, S.M. S., Sprong, H., Rosa, F., Dias, D., 2020. Mitochondrial sequences of *Rhipicephalus* and *Coxiella* endosymbiont reveal evidence of lineages co-cladogenesis. FEMS Microbiol. Ecol. 96, fiaa072 https://doi.org/10.1093/femsec/fiaa072.

Elelu, N., Bankole, A.A., Daphne, H.P., Rabiu, M., Ola-Fadunsin, S.D., Ambali, H.M., Cutler, S.J., 2022. Molecular characterisation of *Rhipicephalus sanguineus* sensu lato ticks from domestic dogs in Nigeria. Vet. Med. Sci. 8, 454–459. https://doi.org/10.1002/vms3.655.

Gray, J., Dantas-Torres, F., Estrada-Pena, A., Levin, M., 2013. Systematics and ecology of the brown dog tick, *Rhipicephalus sanguineus*. Ticks Tick Borne Dis. 4, 171–180. https://doi.org/10.1016/j.ttbdis.2012.12.003.

Guglielmone, A.A., Sánchez, M.E., Franco, L.G., Nava, S., Rueda, L.M., Robbins, R.G., 2015. Hard Ticks (Acari: Ixodida: Ixodidae): a Non-Profit Open-Access Web Portal For Original Descriptions of Tick Species (valid and invalid), Dubious and Uncertain names, and Selected Nomina Nuda. and updates. Instituto Nacional de Tecnologia Agropecuaria, Argentina [available online at: http://rafaela.inta.gob.ar/nombresgarrapatas/ (accessed 27 February 2022)].

Hafez, M., 1981. Biological and Morphological Studies of Tick Populations Identified As *Rhipicephalus sanguineus* in Egypt and Their Potential Relationships to Disease in Humans and animals: Final Report (1975–1980). Dept. of Entomology, Faculty of Science, Cairo University, Egypt.

Hahn, C., Bachmann, L., Chevreux, B., 2013. Reconstructing mitochondrial genomes directly from genomic next-generation sequencing reads–a baiting and iterative mapping approach. Nucleic Acids Res. 41, e129 https://doi.org/10.1093/nar/gkt371.

Hajibabaei, M., Singer, G.A., Hebert, P.D., Hickey, D.A., 2007. DNA barcoding: how it complements taxonomy, molecular phylogenetics and population genetics. Trends Genet. 23, 167–172. https://doi.org/10.1016/j.tig.2007.02.001.

Hansen, H., Bakke, T.A., Bachmann, L., 2007. DNA taxonomy and barcoding of monogenean parasites: lessons from Gyrodactylus. Trends Parasitol. 23, 363–367. https://doi.org/10.1016/j.pt.2007.06.007.

Hekimoglu, O., Saglam, I.K., Ozer, N., Estrada-Pena, A., 2016. New molecular data shed light on the global phylogeny and species limits of the *Rhipicephalus sanguineus* complex. Ticks Tick Borne Dis. 7, 798–807. https://doi.org/10.1016/j.ttbdis.2016.03.014.

Hoogstraal, H., 1956. African Ixodoidea. l. Ticks of the Sudan (With Special Reference to Equatoria Province With Preliminary Reviews of the Genera *Boophilus, Margaropus, Hyaloma*). Department of Medical Zoology, United States Naval Medical Research Unit No. 3., Washington.

Hoogstraal, H., 1958. Notes on African *Haemaphysalis* ticks. IV. Description of Egyptian populations of the yellow dog-tick, *H. leachii leachii* (Audouin, 1827) (Ixodoidea, Ixodidae). J. Parasitol. 44, 548–558. https://doi.org/10.2307/3274429.

Hornok, S., Sándor, A.D., Tomanović, S., Beck, R., D'Amico, G., Kontschán, J., Takács, N., Görföl, T., Bendjeddou, M.L., Földvári, G., Farkas, R., 2017. East and west separation of *Rhipicephalus sanguineus* mitochondrial lineages in the Mediterranean Basin. Parasit. Vectors 10, 39. https://doi.org/10.1186/s13071-017-1985-z.

ICZN, 1999. International Code of Zoological Nomenclature, 4th ed. International Trust for Zoological Nomenclature, London, U.K [available online at. http://www.iczn.org/iczn/index.jsp.].

Kamani, J., 2021. Molecular identification and genetic analysis of *Rhipicephalus sanguineus* sensu lato of dogs in Nigeria, West Africa. Exp. Appl. Acarol. 85, 277–289. https://doi.org/10.1007/s10493-021-00664-w.

Koch, C.L., 1844. Systematische Übersicht über die Ordnung der Zecken. Arch Nat. 10, 217–239. https://doi.org/10.5962/bhl.part.29560.

Liu, G.H., Chen, F., Chen, Y.Z., Song, H.Q., Lin, R.Q., Zhou, D.H., Zhu, X.Q., 2013. Complete mitochondrial genome sequence data provides genetic evidence that the brown dog tick *Rhipicephalus sanguineus* (Acari: ixodidae) represents a species complex. Int. J. Biol. Sci. 9, 361–369. https://doi.org/10.7150/ijbs.6081.

Meiklejohn, K.A., Damaso, N., Robertson, J.M., 2019. Assessment of BOLD and GenBank - their accuracy and reliability for the identification of biological materials. PLoS One 14, e0217084. https://doi.org/10.1371/journal.pone.0217084.

Moraes-Filho, J., Marcili, A., Nieri-Bastos, F.A., Richtzenhain, L.J., Labruna, M.B., 2011. Genetic analysis of ticks belonging to the *Rhipicephalus sanguineus* group in Latin America. Acta Trop. 117, 51–55. https://doi.org/10.1016/j.actatropica.2010.09.006.

Moraes-Filho, J., Krawczak, F.S., Costa, F.B., Soares, J.F., Labruna, M.B., 2015. Comparative evaluation of the vector competence of four South American populations of the *Rhipicephalus sanguineus* group for the bacterium *Ehrlichia canis*, the agent of canine monocytic ehrlichiosis. PLoS One 10, e0139386. https://doi.org/10.1371/journal.pone.0139386.

Morel, P.C., Vassiliades, G., 1962. Les *Rhipicephalus* du groupe sanguineus: espèces africaines (Acariens: Ixodoidea). Rev. Elev. Med. Vet. Pays Trop. 15, 343–386. https://doi.org/10.19182/remvt.7132.

Mumcuoglu, K.Y., Estrada-Pena, A., Tarragona, E.L., Sebastian, P.S., Guglielmone, A.A., Nava, S., 2022. Reestablishment of *Rhipicephalus secundus* Feldman-Muhsam, 1952 (Acari: ixodidae). Ticks Tick Borne Dis. 13, 101897 https://doi.org/10.1016/j.ttbdis.2022.101897.

Nava, S., Beati, L., Venzal, J.M., Labruna, M.B., Szabó, M.P.J., Petney, T., Saracho-Bottero, M.N., Tarragona, E.L., Dantas-Torres, F., Silva, M.M.S., Mangold, A.J., Guglielmone, A.A., Estrada-Peña, A., 2018. *Rhipicephalus sanguineus* (Latreille, 1806): neotype designation, morphological re-description of all parasitic stages and molecular characterization. Ticks Tick Borne Dis. 9, 1573–1585. https://doi.org/10.1016/j.ttbdis.2018.08.001.

Nava, S., Estrada-Peña, A., Petney, T., Beati, L., Labruna, M.B., Szabó, M.P., Venzal, J.M., Mastropaolo, M., Mangold, A.J., Guglielmone, A.A., 2015. The taxonomic status of *Rhipicephalus sanguineus* (Latreille, 1806). Vet. Parasitol. 208, 2–8. https://doi.org/10.1016/j.vetpar.2014.12.021.

Neave, M.J., Mileto, P., Joseph, A., Reid, T.J., Scott, A., Williams, D.T., Keyburn, A.L., 2022. Comparative genomic analysis of the first *Ehrlichia canis* detections in Australia. Ticks Tick Borne Dis. 13, 101909 https://doi.org/10.1016/j.ttbdis.2022.101909.

Ondrejicka, D.A., Locke, S.A., Morey, K., Borisenko, A.V., Hanner, R.H., 2014. Status and prospects of DNA barcoding in medically important parasites and vectors. Trends Parasitol. 30, 582–591. https://doi.org/10.1016/j.pt.2014.09.003.

Ravi, A., Ereqat, S., Al-Jawabreh, A., Abdeen, Z., Abu Shamma, O., Hall, H., Pallen, M.J., Nasereddin, A., 2019. Metagenomic profiling of ticks: identification of novel rickettsial genomes and detection of tick-borne canine parvovirus. PLoS Negl. Trop. Dis. 13, e0006805 https://doi.org/10.1371/journal.pntd.0006805.

Roberts, F., 1965. The taxonomic status of the species of the genera *Rhipicephalus* Koch and *Boophilus* curtice (Acarina: ixodidae) occurring in Australia. Aust. J. Zool. 13, 491–524. https://doi.org/10.1071/ZO9650491.

Šlapeta, J., Chandra, S., Halliday, B., 2021. The "tropical lineage" of the brown dog tick *Rhipicephalus sanguineus* sensu lato identified as *Rhipicephalus linnaei* (Audouin, 1826). Int. J. Parasitol. 51, 431–436. https://doi.org/10.1016/j.ijpara.2021.02.001.

Smith, A.D., Kamiński, M.J., Kanda, K., Sweet, A.D., Betancourt, J.L., Holmgren, C.A., Hempel, E., Alberti, F., Hofreiter, M., 2021. Recovery and analysis of ancient beetle DNA from subfossil packrat middens using high-throughput sequencing. Sci. Rep. 11, 12635. https://doi.org/10.1038/s41598-021-91896-8.

Szabó, M.P., Mangold, A.J., Joao, C.F., Bechara, G.H., Guglielmone, A.A., 2005. Biological and DNA evidence of two dissimilar populations of the *Rhipicephalus sanguineus* tick group (Acari: ixodidae) in South America. Vet. Parasitol. 130, 131–140. https://doi.org/10.1016/j.vetpar.2005.03.008.

Tamura, K., Stecher, G., Kumar, S., 2021. MEGA11: molecular evolutionary genetics analysis version 11. Mol. Biol. Evol. 38, 3022–3027. https://doi.org/10.1093/molbev/msab120.

Walker, J., Keirans, J., Horak, I., 2000. The Genus *Rhipicephalus* (Acari, Ixodidae): A Guide to the Brown Ticks of the World. Cambridge University Press, Cambridge.